Inorganic Chemistry

Article

pubs.acs.org/IC

Deprotonation-Triggered Stokes Shift Fluorescence of an Unexpected Basic-Stable Metal–Organic Framework

Nian Zhao,[†] Fuxing Sun,[†] Shixing Zhang,[†] Hongming He,[†] Jia Liu,[‡] Qin Li,[§] and Guangshan Zhu*[,†,‡]

[†]State Key Laboratory of Inorganic Synthesis and Preparative Chemistry, College of Chemistry and [‡]Department of Chemistry, Jilin University, Changchun 130012, China

[§]Queensland Micro- and Nanotechnology Center, Griffith University, Queensland 4111, Australia

Supporting Information

ABSTRACT: A new three-dimensional porous metal–organic framework, JUC-119, constructed by a pyrene-based dendritic organic linker, H_8TIAPy (H_8TIAPy = 1,3,6,8-tetrakis(3,5-isophthalic acid)pyrene), and Eu(III) has been synthesized successfully. JUC-119 shows unexpected stability under a wide range of basic conditions from 0 to 0.01 M NaOH. Furthermore, with two carboxyl groups uncoordinated in each ligand, the crystals of JUC-119 show deprotonation-triggered Stokes shift fluorescence under basic conditions. As the concentration of base increases from 0 to 0.01 M NaOH, the luminescence emission of JUC-119 becomes gradually red shifted from 455 to 485 nm. In addition, the Stokes shift shows a good linear relationship to $-\log[OH^-]$, which makes JUC-119 promising for base sensing.

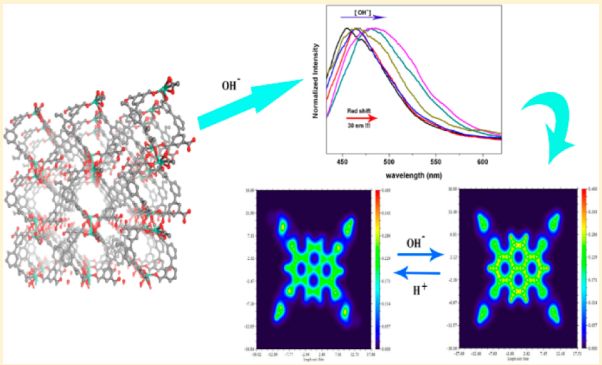

INTRODUCTION

Metal–organic frameworks (MOFs) constructed by ligands with chromophores have received considerable attention, primarily because of their potential applications as chemical sensors.[1] Designing and synthesizing MOF-based chemical sensors, especially for detecting gaseous analytes,[2] are advantageous, as MOFs have high internal surface areas and large solvent-accessible cavities[3] that are favored for concentrating gaseous analytes to levels high above those in the surrounding atmosphere, thus lowering the limit of detection.

The most common method of detection in luminescent MOF-based sensors is a change in fluorescence intensity. In MOFs, analyte molecules quench the excited states of rare earth ions[4] or fluorescent linkers,[5] thereby turning off or reducing the luminescence intensity of parent materials, which is known as the turn-off mechanism. The detection of many volatile[6] and explosive substances[7] with luminescent MOFs is based on this mechanism. More desirable and easily detectable are turn-on mechanisms, where the presence of the specific analyte triggers an increase in the luminescence intensity from a completely dark off state to a highly emissive one. The most famous example of this is aggregation-induced emission (AIE),[8] where the molecules are nonemissive in the default state, and the fluorescence of such molecules is turned on when they aggregate in a solid or colloidal state.

Another method of detection used in MOF-based sensors is a Stokes shift in the emission wavelength, which is easier and more intuitive to detect. The interaction between analyte molecules and the fluorescent organic linkers could change the energy level, electron distribution, or conjugacy of the latter; thus, fluorescence emission can have a red or blue shift. These analytes can be solvent molecules,[9] metal ions,[10] and so on. Detecting H^+ or OH^- with organometallic compounds[11] is common; however, there are few examples of this in the MOF field, mostly because of the instability of MOFs under acidic or basic conditions. Recently, Zhou et al. reported a superstable porphyrin Zr-MOF with pH-dependent fluorescent intensity.[12] The fluorescent intensity changes according to the concentration of acid or base caused by the protonation and deprotonation of N atoms in the porphyrin ring. However, to the best of our knowledge, Stokes shift luminescence induced by deprotonation has not been described. In addition, detecting H^+ or OH^- in aqueous solution is very common, and instruments to do so are widely available; however, reports of detecting them in organic solvents are rare.

Herein, we report a luminescent MOF, JUC-119, constructed with Eu (III) and H_8TIAPy (Scheme 1), a dendritic ligand with a pyrene chromophore that we reported in previous work.[13] Furthermore, JUC-119 can be well-maintained under a wide range of basic conditions, and it shows Stokes shift luminescence emission when increasing the concentration of OH^- in solution to a limited extent. To our knowledge, JUC-119 is the first MOF exhibiting base-dependent Stokes shift luminescence. Its good base resistance and linear fluorescence response to the concentration of base make JUC-119 promising for OH^- detection.

Received: July 1, 2014
Published: December 9, 2014

Scheme 1. H_8TIAPy Ligand and the Octahedral Conformation in JUC-119

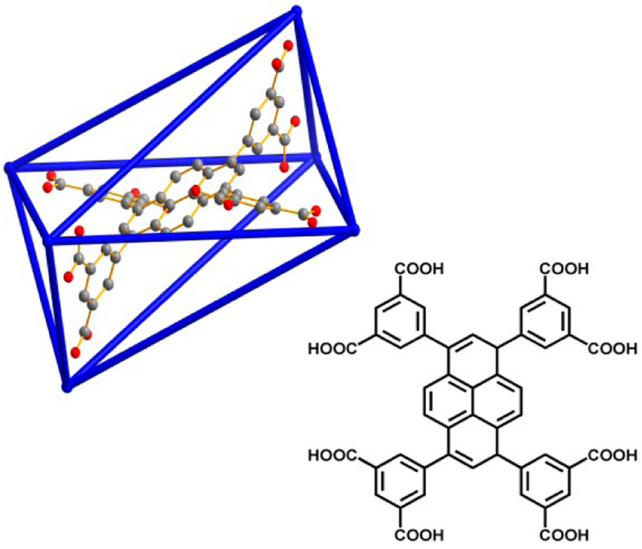

RESULTS AND DISCUSSION

The synthesis of H_8TIAPy was performed according to our previous work.[13] The reaction of H_8TIAPy with $Eu(NO_3)_3$ in an acidic solvent mixture of DMF/H_2O = 5:1 at 85 °C for about 2 days gave yellow block crystals of JUC-119, formulated as $[Eu_2(H_2TIAPy)\cdot(H_2O)_4]\cdot$(guest), with good yield. Single-crystal X-ray analysis revealed that JUC-119 crystallized in the triclinic space group $P\bar{1}$ with lattice parameters a = 10.218 Å, b = 11.517 Å, c = 16.312 Å, α = 82.7°, β = 75.9°, and γ = 77.5°. There are two unique Eu atoms in the asymmetric unit. Both of them are coordinated by two terminal water molecules and five carboxyl groups of the ligand, among which two are monodentate, one is bidentate, and the other two are bidentate with a μ2−O to form a Eu_2 cluster (Figure 1a). Each ligand connects to six Eu_2 clusters, and of the eight carboxyl groups, two remain uncoordinated (Figure 1b). The assembling of the clusters and the organic linkers forms a porous three-dimensional framework, with a solvent-accessible pore volume as high as 52.3%, calculated by PLATON. There are two kinds of channels in the [100] direction, one is about 10 × 8 Å (Figure 1c and Figure S1, Supporting Information), and the other one is filled with the uncoordinated carboxyl groups of the ligand (Figure 1d). The interior of the channels in JUC-119 contains disordered guest molecules, and attempts to locate them failed. Topology analysis of the framework was conducted by TOPOS 4.0 program. Both the Eu_2 cluster and the linker could be simplified as a six-connected node; thus, the whole framework of JUC-119 could be simplified as a (6,6)-connected **pcu** net (Figure 1e), which is the same as MOF-5. Each primitive cube in MOF-5 comprises eight Zn_4O clusters as vertexes and 12 linkers as edges; however, in JUC-119, four Eu_2 clusters and four pyrenes of the ligands function as vertexes, and the benzene rings of the ligand act as edges (Figure 1f and Supporting Information, Figure S2). Thermogravimetric analyses (TGA) showed that JUC-119 started to decompose around 300 °C, and the weight loss before 250 °C could be mainly attributed to the isolated guest molecules in the channels and coordinated water molecules (Supporting Information, Figure S4). Phase purity could be confirmed by the similarity between the simulated and experimental X-ray diffraction patterns (Supporting Information, Figure S3).

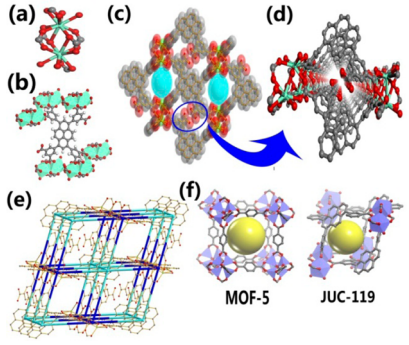

Figure 1. (a) Coordination mode of an Eu_2 cluster in JUC-119. (b) Coordination mode of H_8TIAPy in JUC-119. (c) A channel from the [100] direction of JUC-119. (d) Uncoordinated carboxyl groups in the channel. (e) **pcu** topology of JUC-119. (f) Primitive cubes of MOF-5 and JUC-119. Gray atoms are C, red are O, and green are Eu.

To study the stability further, we soaked crystals of JUC-119 under basic conditions to test its resistance to base. An equal amount of JUC-119 crystals were soaked in a series of concentrations of NaOH in EtOH for 1 day, and then powder X-ray diffraction (PXRD) measurements were conducted. It was found that the crystallinity of JUC-119 can be maintained under a large range of basic conditions from 0 to 10 mM NaOH. However, further increasing the concentration of base led to a collapse of the framework (Figure 2). This unexpected base resistance might be related to the gradual deprotonation process of JUC-119. A gradual disappearing of the −OH group's stretching vibration peak at about 2930 cm^{-1} in the IR spectrum confirmed the deprotonation process (Supporting Information, Figure S5). It is likely that JUC-119 is first deprotonated to become anionic in the NaOH/EtOH solution until all uncoordinated carboxyl groups are deprotonated and then the excess NaOH attacks the framework, leading to the rapid collapse.

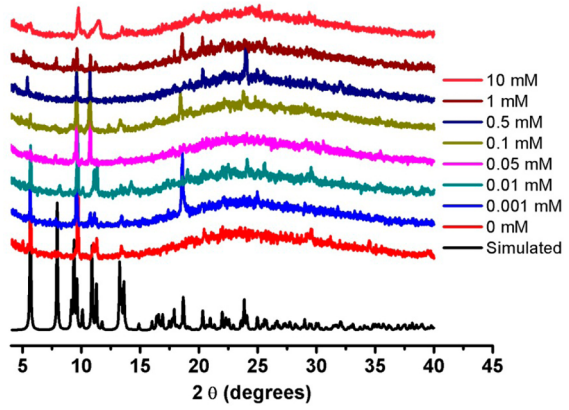

Figure 2. PXRD of JUC-119 in an EtOH solution with different NaOH concentrations.

Given the pyrene choromphore in the ligand, we monitored the change of fluorescence of JUC-119 in different concentrations of NaOH in a solution of EtOH. The fluorescence emission of the solution without NaOH was at 455 nm (λ = 397 nm). When the NaOH concentration was 0.001 mM, the maximum emission showed a slight red shift to 459 nm. As the

dx.doi.org/10.1021/ic501560z | Inorg. Chem. 2015, 54, 65−68

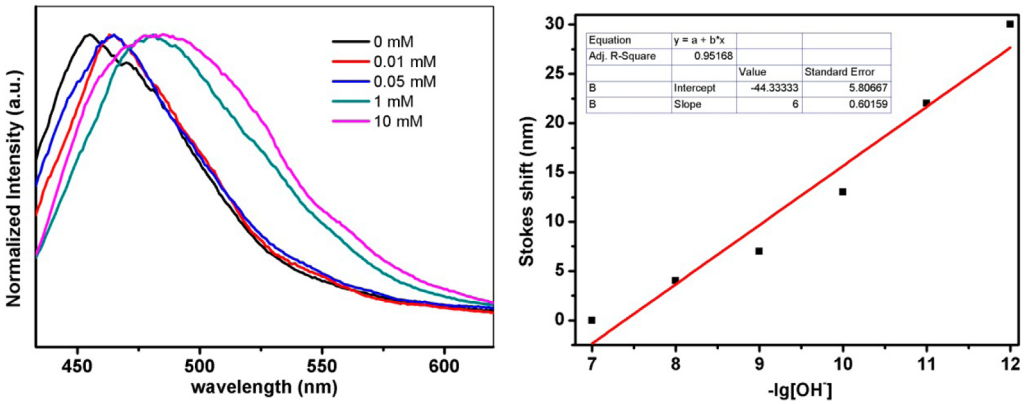

Figure 3. Fluorescence emission of JUC-119 in EtOH solution with different NaOH concentrations (left) and the linear relationship between the Stokes shift and the $-\log[OH^-]$ value of the solution (right).

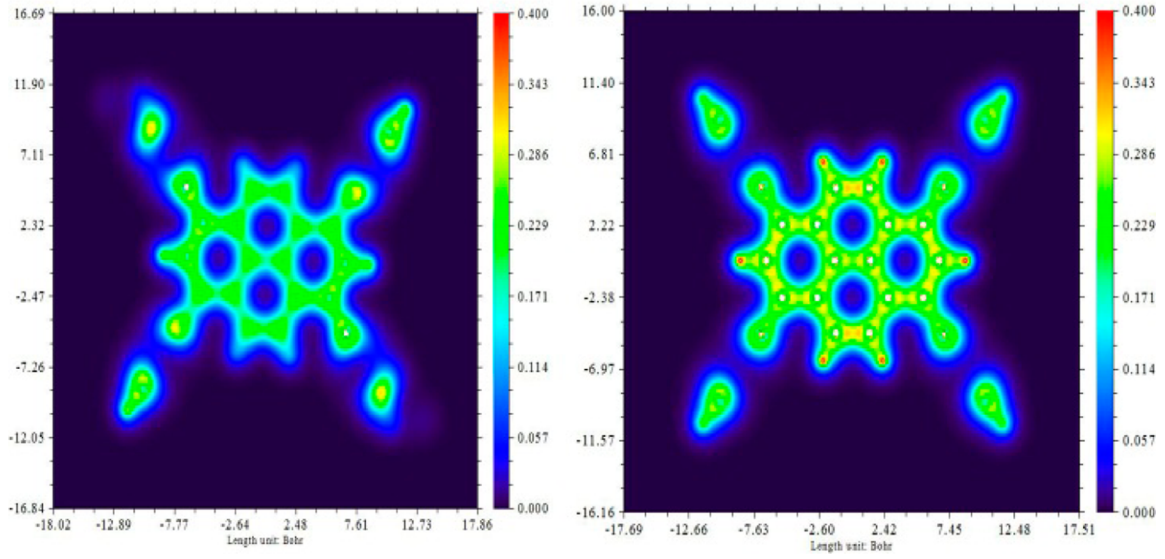

Figure 4. Electron density maps of H_2TIAPy^{6-} (left) and $TIAPy^{8-}$ (right) constrained in JUC-119 in the pyrene plane.

concentration of NaOH increased, the maximum emission of the solution gradually red shifted to 485 nm when the NaOH concentration was as high as 10 mM. During the whole base-dependent experiment, the total Stokes shift was up to 30 nm! Moreover, we found that the Stokes shift had a good linear relationship with the $-\log[OH^-]$ value of the solution (Figure 3). To check the repeatability of the sensor, we titrated 2 M HCl to decrease the NaOH concentration from 10 to 0.001 mM, and the corresponding fluorescence emission was recorded. The maximum fluorescence emission gradually shifted back from 485 to 461 nm, which confirmed the reversibility of base sensing (Supporting Information, Figure S8). Good base resistance and the linear fluorescence response to the concentration of base make JUC-119 promising for base sensing.

To explore the mechanism of this base-dependent fluorescence, density functional theory (DFT) was used to compare the electron density distribution of the ligand before (H_2TIAPy^{6-}⊂JUC-119) and after deprotonation ($TIAPy^{8-}$⊂JUC-119). The theoretical calculation was performed with Gaussian 09 on the platform of Ubuntu. The basis set chosen was 6-31g(d), and the DFT function was B3LYP. The conformation of the ligand was directly picked out from the crystal structure, and all dihedral angles between the pyrene and benzene were fixed. Electron density analyses were conducted via the free quantum chemistry software *Multiwfn*[14] and are displayed as visualized plots for analysis. The occupation number of inner orbitals for all atoms was set to zero to avoid interference by inner electrons, and the pyrene plane was chosen to be the projection plane. Clearly, the color of the electron density plot was remarkably deepened from green to yellow after the ligand was deprotonated, which indicates an increase in the electron density of the chromophore (Figure 4). According to experimental data and quantum chemistry analysis, the base-dependent Stokes shift luminescence might be because of −COOH groups, which are strongly electron-withdrawing; once they are deprotonated to $-COO^-$ groups, they become strongly electron-donating, increasing the electron density of pyrene and lowering the energy gap. Thus, the crystals showed a base-dependent red shift in their fluorescence emission.

CONCLUSIONS

A porous Eu-MOF, JUC-119, constructed by a dendritic pyrene-based ligand, H_8TIAPy, with a (6,6)-connected **pcu** net has been investigated. JUC-119 shows unexpected stability in EtOH solution under a large range of NaOH concentrations, from 0 to 0.01 M. In addition, with two uncoordinated carboxyl

dx.doi.org/10.1021/ic501560z | *Inorg. Chem.* 2015, 54, 65−68

groups in each ligand, JUC-119 also shows a deprontonation-triggered Stokes shift in fluorescence emission from 455 to 485 nm. Moreover, the Stokes shift shows a good linear relationship with the $-\log[OH^-]$ value of the solution. Sensor repeatability was confirmed by titrating HCl, in which the fluorescence emission of the solution shifted back as the concentration of base decreased from 0.01 to 0 M. A possible mechanism of this deprotonation-triggered Stokes shift in fluorescence was investigated with the aid of theoretical calculations. Good base resistance and a linear fluorescence response to base make this MOF promising for base sensing.

EXPERIMENTAL SECTION

Materials and Methods. All reagents and solvents for the syntheses were purchased from commercial sources and used as received, except for H_8TIAPy, which was synthesized according to our previous work.[13] Powder X-ray diffraction (PXRD) measurements were performed on a Rigaku DMAX 2550 diffractometer at 50 kV, 20 mA with Cu Kα (λ = 1.5418 Å). Thermogravimetric analysis (TGA) was performed on a PekinElmer thermogravimetric analyzer with a heating rate of 5 °C/min. Fluorescence measurement was performed on FLUOROMAX-4 spectrometer. UV−vis spectroscopy was performed with a U-4200 spectrophotometer.

Synthesis of JUC-119. H_8TIAPy (5 mg, 0.0058 mmol), $Eu(NO_3)_3$ (15 mg, 0.0444 mmol), DMF (5 mL), H_2O (0.7 mL), and concentrated HNO_3 (0.3 mL) were combined in a 20 mL glass vial, sealed, and heated at 85 °C for 24 h and then cooled to room temperature. Yellow block crystals were collected and air-dried (yield: 80%, based on H_8TIAPy). Elemental and ICP analysis for $Eu_2(H_2TIAPy)\cdot(H_2O)_4$ = $C_{48}H_{28}O_{20}Eu_2$ calcd (%): C, 46.91; H, 2.28; Eu, 50.81. Found (%): C, 47.02; H, 2.11; Eu, 50.87.

Single-Crystal X-ray Crystallography. Single-crystal X-ray diffraction data were collected using a Bruker-AXS SMART APEX2 CCD diffractometer (Mo Kα, λ = 0.710 73 Å). Indexing was performed using APEX2 (difference vectors method). Data integration and reduction were performed using SaintPlus. Absorption correction was performed by multiscan method implemented in SADABS. Space groups were determined using XPREP implemented in APEX2. Structures were solved using SHELXL-97 (direct methods) and refined using SHELXL-97 (full-matrix least-squares on F^2) with anisotropic displacement contained in the APEX2 program package. Hydrogen atoms on carbon and nitrogen were calculated in ideal positions with isotropic placement parameters set to 1.2 × U_{eq} of the attached atoms, whereas hydrogens of water molecules were not added into the structure. In the structure, free solvent molecules were highly disordered, and attempts to locate and refine the solvent peaks were not successful. Contributions to scattering due to these solvent molecules were removed using the SQUEEZE routine of PLATON, and the structures were then refined again using the data generated. The contents of the solvent region are not represented in the unit cell contents in the crystal data. Crystallographic data and structural refinements for JUC-119 are summarized in Table S1 (Supporting Information).

ASSOCIATED CONTENT

Supporting Information

Crystal structure representation, PXRD, UV−vis spectra, TGA and fluorescence spectra, crystal structure data, and CIF files of JUC-119. This material is available free of charge via the Internet at http://pubs.acs.org. Crystallographic data for this article was deposited with the Cambridge Crystallographic Data Centre (CCDC) as entry CCDC 990747.

AUTHOR INFORMATION

Corresponding Author

*E-mail: zhugs@jlu.edu.cn.

Notes

The authors declare no competing financial interest.

ACKNOWLEDGMENTS

The authors thank the National Basic Research Program of China (973 Program, Grant Nos. 2012CB821700 and 2014CB931804), the Major International (Regional) Joint Research Project of NSFC (Grant No. 21120102034), and the NSFC (Grant No. 20831002) for financial support.

REFERENCES

(1) (a) Achmann, S.; Hagen, G.; Kita, J.; Malkowsky, I. M.; Kiener, C.; Moos, R. *Sensors* **2009**, *9*, 1574−1589. (b) Khoshaman, A. H.; Bahreyni, B. *Sens. Actuators, B* **2012**, *162*, 114−119.

(2) (a) Khoshaman, A. H.; Bahreyni, B. *IEEE Sens.* **2011**, *23*, 1101−1104. (b) Kreno, L. E.; Hupp, J. T.; Van Duyne, R. P. *Anal. Chem.* **2010**, *82*, 8042−8046. (c) Dong, M. J.; Zhao, M.; Ou, S.; Zou, C.; Wu, C. D. *Angew. Chem., Int. Ed.* **2014**, *53*, 1575−1579.

(3) Murray, L. J.; Dinca, M.; Long, J. R. *Chem. Soc. Rev.* **2009**, *38*, 1294−1314.

(4) (a) Liu, B. X.; Chen, Y. *Anal. Chem.* **2013**, *85*, 11020−11025. (b) Rocha, J.; Carlos, L. D.; Paz, F. D.; Ananias, D. *Chem. Soc. Rev.* **2011**, *40*, 926−940. (c) Zheng, M.; Tan, H. Q.; Xie, Z. G.; Zhang, L. G.; Jing, X. B.; Sun, Z. C. *ACS Appl. Mater. Interfaces* **2013**, *5*, 1078−1083.

(5) (a) Saha, R.; Joarder, B.; Roy, A. S.; Islam, S. M.; Kumar, S. *Chem.—Eur. J.* **2013**, *19*, 16607−16614. (b) Wei, N.; Zhang, Y. R.; Han, Z. B. *CrystEngComm* **2013**, *15*, 8883−8886. (c) Tian, D.; Li, Y.; Chen, Y. R.; Chang, Z.; Wang, G. Y.; Bu, X. H. *J. Mater. Chem. A* **2014**, *2*, 1465−1470.

(6) (a) Yu, Y.; Zhang, X. M.; Ma, J. P.; Liu, Q. K.; Wang, P.; Dong, Y. B. *Chem. Commun.* **2014**, *50*, 1444−1446. (b) Xu, N.; Yang, J.; He, Y. C.; Liu, Y. Y.; Ma, J. F. *CrystEngComm* **2013**, *15*, 7360−7371. (c) Zhou, X. H.; Li, L.; Li, H. H.; Li, A.; Yang, T.; Huang, W. *Dalton Trans.* **2013**, *42*, 12403−12409.

(7) (a) Ma, D. X.; Li, B. Y.; Zhou, X. J.; Zhou, Q.; Liu, K.; Zeng, G.; Li, G. H.; Shi, Z.; Feng, S. H. *Chem. Commun.* **2013**, *49*, 8964−8966. (b) Lee, J. H.; Kang, S.; Lee, J. Y.; Jaworski, J.; Jung, J. H. *Chem.—Eur. J.* **2013**, *19*, 16665−16671. (c) Wang, Y. P.; Wang, F.; Luo, D. F.; Zhou, L.; Wen, L. L. *Inorg. Chem. Commun.* **2012**, *19*, 43−46.

(8) (a) Shustova, N. B.; McCarthy, B. D.; Dinca, M. *J. Am. Chem. Soc.* **2011**, *133*, 20126−20129. (b) Shustova, N. B.; Cozzolino, A. F.; Dinca, M. *J. Am. Chem. Soc.* **2012**, *134*, 19596−19599.

(9) (a) Wang, J. H.; Li, M.; Li, D. *Chem. Sci.* **2013**, *4*, 1793−1801. (b) Takashima, Y.; Martinez, V. M.; Furukawa, S.; Kondo, M.; Shimomura, S.; Uehara, H.; Nakahama, M.; Sugimoto, K.; Kitagawa, S. *Nat. Commun.* **2011**, *2*, 168.

(10) Shahat, A.; Hassan, H. M. A.; Azzazy, H. M. E. *Anal. Chim. Acta* **2013**, *793*, 90−98.

(11) (a) Kobayashi, N.; Kamei, Y.; Shichibu, Y.; Konishi, K. *J. Am. Chem. Soc.* **2013**, *135*, 16078−16081. (b) Grusenmeyer, T. A.; Chen, J.; Jin, Y.; Nguyen, J.; Rack, J. J.; Schmehl, R. H. *J. Am. Chem. Soc.* **2012**, *134*, 7497−7506. (c) Li, D.; Song, J.; Yin, P. C.; Simotwo, S.; Bassler, A. J.; Aung, Y. Y.; Roberts, J. E.; Hardcastle, K. I.; Hill, C. L.; Liu, T. B. *J. Am. Chem. Soc.* **2011**, *133*, 14010−14016. (d) Moore, J. D.; Lord, R. D.; Cisneros, G. A.; Allen, M. J. *J. Am. Chem. Soc.* **2012**, *134*, 17372−17375.

(12) Jiang, H. L.; Feng, D. W.; Wang, K. C.; Gu, Z. Y.; Wei, Z. W.; Chen, Y. P.; Zhou, H. C. *J. Am. Chem. Soc.* **2013**, *135*, 13934−13938.

(13) Zhao, N.; Sun, F. X.; He, H. M.; Jia, J. T.; Zhu, G. S. *Cryst. Growth Des.* **2014**, *14*, 1738−1743.

(14) (a) Lu, T.; Chen, F. W. *J. Comput. Chem.* **2012**, *33*, 580−592. (b) Lu, T.; Chen, F. W. *J. Mol. Graphics Modell.* **2012**, *38*, 314−323.